ENERGY SCIENCE AND TECHNOLOGY
Vol. 1, No. 1, 2011 PP. 49-63
ISSN 1923-8460 [PRINT]
ISSN 1923-8479 [ONLINE]

CSCanada
www.cscanada.net
www.cscanada.org

Performance of a Solar Chimney Under Egyptian Weather Conditions:

Numerical Simulation and Experimental Validation

A. A. Mostafa[1]
M. F. Sedrak[1]
Adel M. Abdel Dayem[1,*]

[1] Dept. of Mech. Power Eng., Faculty of Eng. (Mattaria), Masaken El-Helmia P. O. 11718, Cairo, Egypt.

* Corresponding author. Email: adel_abdeldayem@hotmail.com

Abstract: High solar radiation and ambient temperature, and large desert in Egypt are excellent conditions to install efficiently solar chimney power plants there. Therefore this research aimed to develop a validated mathematical model and governing equations of solar chimney. It is proposed to improve the performance of solar chimney under effects of various parameters, and study of possibility of installing solar chimney in Egypt. The mathematical simulation of the solar chimney has been developed including all its performance parameters, dimensions (of collector, chimney and turbine) and the metrological data; which were considered as inputs of the simulation program. A comparison between the mathematical and experimental performance has been investigated to validate the mathematical simulation. The mathematical model has been used to predict the performance of the solar chimney power plant over a year in Egypt. It is used to study of effects of geometrical parameters, and investigate possibility of the optimum geometrical dimensions. It is obtained that there is in fact no optimum physical size for such plants without considering the economical constraints. The chimney height has a significant effect in the chimney performance. Visualizing of annual performance of the solar chimney would seem to be essentially a power generator in Egypt if it installed in a large scale.

Key words: Solar chimney; Numerical simulation; Annual performance; Experimental validation; Optimization

† Received 10 February 2011; accepted 26 February 2011.

Nomenclature

A	Area, [m^2]	p_t	Pressure drop across the turbine [Pa]
C, cp	Specific heat [kJ/kg.K]	P	Power [W]
c_w	Coefficient of friction due to surface shear stress $= \frac{\tau_w}{\rho V^2/2}$	Pr	Prandtl number $= \frac{c_p \mu}{k}$
F	Friction coefficient due to pressure drop for internal flow $= \frac{\Delta p}{(L/D)(\rho u^2/2)}$	q''	Heat transferred to air stream [W/m^2]
G	Gravitational acceleration 9.81 [m/s^2]	r, x	Radial distance [m]
H	Heat transfer convection coefficient [W/m^2K]	R	Ideal gas constant, 287.05 [J /kg K]
h_r	Radiation heat transfer coefficient [W/m^2K]	Ra	Rayleigh number $= \frac{g(1/T_f)(T_s - T_\infty)L_c^3}{\upsilon^2}$
h_{rlg}	Ground-cover radiation heat transfer coefficient [W/m^2K]	Re_x	Reynolds number for flow over flat plate $= \frac{Vx}{\upsilon}$
h_{rs}	Sky radiation heat transfer coefficient [W/m^2K]	Re_D	Reynolds number for flow through circular tube $= \frac{VD}{\upsilon}$
h_w	Wind convection heat transfer [W/m^2K]	R_{ch}	Chimney radius [m]
H_o	chimney height [m]	R_{coll}	Collector radius [m]
I_{tot}	Solar radiation [W/m^2]	S	Absorbed solar radiation [W/m^2]
K	Thermal conductivity [W/m K]	t	Time [s]
$\dot{m}$	Mass flow rate of air [kg/s]	T	Temperature, K or ^oC
Nu	Nusselt number $= \frac{hL}{k}$	U	Overall heat transfer coefficient [$W/m^2\ K^1$]
p_l	Friction pressure loss [Pa]	u,w	Velocity of air under collector, upwind velocity [m/s]
p_p	Total potential pressure difference in the chimney [Pa]		

Greek Symbol

α	Absorptivity	σ	Stefan–Boltzmann constant, 5.67 x 10^{-8} [W/m^2K^4]
ε	Emissivity	τ	Shear stress [Pa]
η_{coll} , $\eta_{overall}$	Collector efficiency, overall efficiency [%]	τ_{coll}	Transmittance of plastic cover
ρ, ρ_o, ρ_t	Air density, ambient air density, air density inside chimney [kg/m^3]		

Subscripts

1,2	See Fig. 2	f	fluid	m	mean	s	Sky
b	Bottom	g	ground	o	Outlet	X	Variable
coll	collector	i	inlet	*r*	radiation	w	wall

1. INTRODUCTION

In solar chimney, air is heated by solar radiation under a low circular glass roof open at the periphery; this and the natural ground below it form a hot air collector. In the middle of the roof is a vertical chimney with large air inlet at its base. The joint between the roof and the chimney base is airtight. As hot air is lighter than cold air it rises up the chimney. Suction from the chimney then draws in more hot air from the collector, and cold air comes in from the outer perimeter. Continuous 24 hours-operations is possible by placing tight water-filled tubes under the roof. The water heats up during daytime and emits its heat at night. These tubes are filled only once, no further water is needed. Thus solar radiation causes a constant updraft in the chimney. The energy is converted into mechanical energy by pressure-staged wind turbines at the base of the chimney, and into electrical energy by conventional generators.

The productivity of solar chimney power plant depends on many factors. They are grouped in basic geometrical parameters such as collector radius, chimney height, chimney radius, canopy (absorber) height, which is the height of collector cover from ground, climate conditions, physical and mechanical properties of the different components, and turbine characteristics.

The first large-scale 200 MW solar chimney power plant in the world was commissioned at 1982 in Manzanares – Spain with a great potential of such power plant. From that date many small-scale plants were installed, the most of research work in that area is a numerical simulation due to high initial cost of such plants. The small-scale plants cannot give enough power to rotate a practical plant. Economic appraisals based on experience and knowledge gathered so far have shown that even solar chimneys rated at 100 and 200 MW are capable of generating energy at costs comparable to those of conventional power plants [1]. Accordingly Mullett [2] developed a numerical analysis for the solar chimney of solar chimney at Manzanares, Spain. He showed that, the overall efficiency was directly related to the height of the chimney and is shown to be about l% for a height of 1000 m. In addition Pasumarthi et al. [3] validated a numerical simulation of Manzanares plant within 20% in the exit velocity, and within 9.5% of the electric power output was attained. On that way, Bilgen et al. [4] showed that solar chimney power plants at high latitudes may had satisfactory thermal performance and produce as much as 85% of the same plants in southern locations with horizontal collector field. The overall thermal performance of these plants was a little less than 0.5%.

A numerical simulation was performed by Tingzhen et al. [5] to analyze the characteristics of heat transfer and air flow in the solar chimney power plant system. They showed that the relative static pressure decreased while the velocity increased significantly inside the system with the increase of solar radiation. Moreover, Gannon et al. [6], Fluri et al. [7] and Tingzhen et al. [5] developed such validated model. Padki et al. [8] applied the continuity, momentum and energy equations in differential form. The predictions of the analytical model showed to be in good agreement with those of the differential model, and the percentage error in the predictions of the analytical model was shown to be of the order of 4-6%.

Regarding the effect of chimney geometry on the performance, Bernardes et al. [9] developed a validated mathematical model to estimate the temperature and power output of solar chimneys. The maximum power can be reached when the factor pressure drop at the turbine is equal to approximately 0.97 from the total potential pressure. Other parameters were also involved in the study such as; distance between absorber and ground, double cover area, water-storage system area and thickness. The results showed that their effect was insignificant since the energy output was the same. Similarly, Backström et al. [10] found that maximum fluid power was available at

much lower flow rate and much higher turbine pressure drop than the constant pressure potential assumption given.

Moreover Maia et al. [11] presented a validated numerical simulation showed that the height and diameter of the tower were the most significant physical variables for solar chimney design. The maximum chimney height for convection avoiding negative buoyancy at the latter chimney and the optimal chimney height for maximum power output were presented and analyzed by Zhou et al. [12] using a theoretical model validated with the measurements of the prototype in Manzanares. The results showed that maximum height gradually increased with the lapse rate increasing and go to infinity at a value of around 0.0098 K/ m.

From the above presentation, it is obviously explained that the mathematical model governed by analytical analysis can be used with good performance prediction. The current study will combine the analysis of optimal ratio of turbine pressure drop to available pressure drop in a solar chimney power plant for maximum fluid power.

2. MATHEMATICAL MODEL

As shown in Fig. 1 the chimney consists of main elements, collector, turbine and chimney. A mathematical model is developed including those elements. The analysis used in this study is based on the following simplifying assumptions:

a) Axisymmetric flow of the air in the collector, i.e., non-uniform heating of the collector surface in terms of the sun's altitude angle is neglected;
b) The collector is placed over a plan surface;
c) Constant height of collector element i.e. radial inward flow between two parallel plates;
d) The heat losses through the wall of the chimney are neglected; and the flowing humid air is considered as a mixture of two ideal gases.

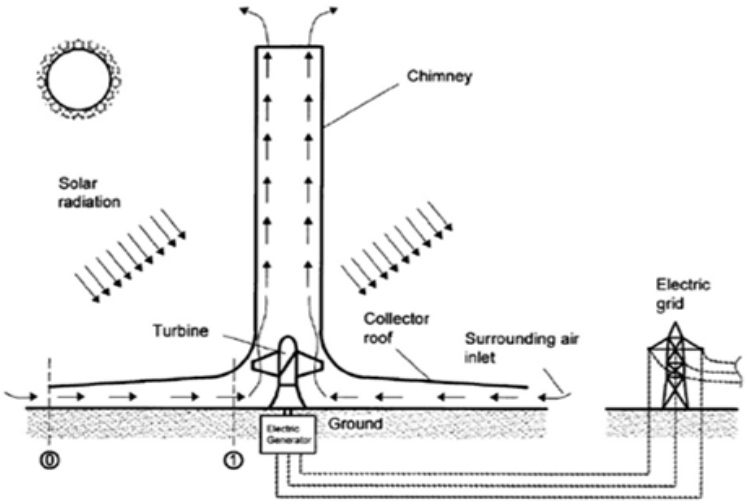

Fig. 1: Principle of the solar chimney: glass roof collector, chimney tube, wind turbines

2.1 Collector

The collector is considered as radial flow between two parallel plates. Applying the momentum equation across a differential section of the collector as can be obtained from Fig. 2 yields:

$$\frac{\partial(mu)}{\partial t} = -\dot{m}u_2 + \dot{m}u_1 + p_1A_1 - p_2A_2 - 2\pi r_c \Delta r \tau \quad (1)$$

Correlations employed for the shear stress in the collector (flat plate) [13].

$$\tau = c_w \frac{1}{2} \rho u^2 \Delta x \tag{2}$$

where

$$c_w = \frac{1.292}{\sqrt{Re_x}}$$

At laminar, smooth, $Re_x < 5 \times 10^5$

$$c_w = \frac{0.0592}{\sqrt[5]{Re_x}}$$

At turbulence, smooth, $5 \times 10^5 < Re_x < 10^7$

$$c_w = \frac{0.074}{\sqrt[5]{Re_x}} - \frac{1742}{Re_x}$$

At transition, smooth, it is used C_w for turbulent flow with $Re_x = 5 \times 10^5$.

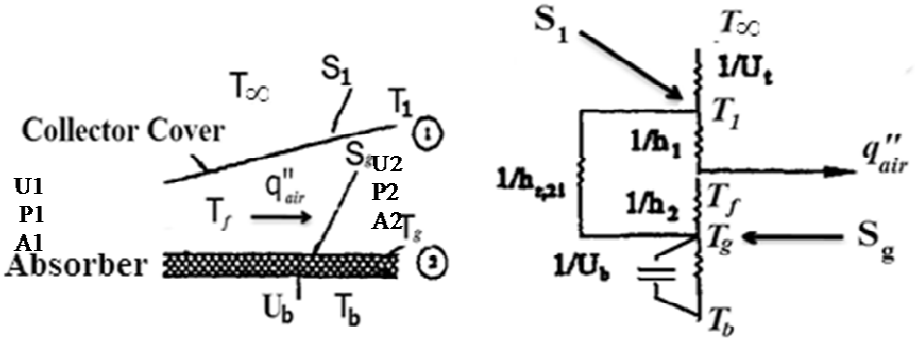

Fig. 2: Collector with single cover and its thermal network

The following heat balance equations are obtained from the thermal network as shown in Fig. 2 at the points considering the thermal contact resistance:

$$\text{Cover:} \quad S_1 = U_t (T_1 - T_\infty) + h_{r1g} (T_1 - T_g) + h_1 (T_1 - T_f) \tag{3}$$

$$\text{Fluid:} \quad h_1 (T_1 - T_f) + h_2 (T_g - T_f) = q''_{air} \tag{4}$$

$$\text{Ground (absorber):} \quad S_g + h_{r1g} (T_1 - T_g) = U_b (T_g - T_b) + h_2 (T_g - T_f) \tag{5}$$

Where, T_f is the mean temperature of the flow element under the collector. The useful energy absorbed by moving air can be written in terms of the mean fluid and inlet temperature as:

$$q''_{air} = \frac{\dot{m} c_p}{A} (T_{fo} - T_{fi}) = \frac{2\dot{m} c_p}{A} (T_f - T_{f,i}) \tag{6}$$

2.2 Heat Transfer Coefficients

The overall top heat loss coefficient may be obtained from

$$U_t = (h_w + h_{rs}) \tag{7}$$

With

$$h_w = \frac{k}{\Delta x} Nu \tag{8}$$

And

$$h_{rs} = \frac{\sigma\varepsilon\,(T_1 + T_s)(T_1^{\,2} + T_s^{\,2})(T_1 - T_s)}{(T_1 - T_\infty)} \tag{9}$$

The clean sky temperature T_s is given by Bernardes et al [1] as:

$$T_s = T_\infty \left[\begin{array}{l} 0.711 + 0.0056\,(T_{dp} - 273.15) \\ + 0.000073\,(T_{dp} - 273.15)^2 + 0.013\cos(15t) \end{array} \right]^{0.25} \tag{10}$$

Where t is the time in hours from midnight. The ground heat transfer coefficient is given by:

$$U_b = \frac{2b}{\sqrt{\pi t}} \tag{11}$$

With

$$b = \sqrt{k\rho c_p} \tag{12}$$

Where t in Eq. (11) is the time in seconds from sunrise. The radiation heat transfer coefficients between the cover and ground or absorber.

$$h_{r1g} = \frac{\sigma\,(T_1^{\,2} + T_g^{\,2})(T_1 + T_g)}{\left(\frac{1}{\varepsilon_1} + \frac{1}{\varepsilon_g} - 1 \right)} \tag{13}$$

The solar radiation heat fluxes absorbed by cover

$$S_1 = \alpha_c I_{tot} \tag{14}$$

The solar radiation heat fluxes absorbed by ground or absorber

$$S_g = \tau_{\text{cover}} \cdot \alpha_{absorber} \cdot I_{tot} \tag{15}$$

By substituting Eq. (5) into Eq. (3) and rearranging we obtain:

$$\begin{bmatrix} (U_t + h_{r1g} + h_1) & -h_1 & -h_{r1g} \\ h_1 & -\left(h_1 + h_2 + \frac{2\dot{m}c_p}{A}\right) & h_2 \\ h_{r1g} & h_2 & -(h_{r1g} + h_2 + U_b) \end{bmatrix} \begin{bmatrix} T_1 \\ T_f \\ T_g \end{bmatrix} = \begin{bmatrix} S_1 + U_t T_\infty \\ -\frac{2\dot{m}c_p}{A} T_{f,i} \\ -(U_b T_b + S_g) \end{bmatrix} \quad (16)$$

Regarding Eq. (16) temperatures T_1, T_f and T_g are the only unknowns if h_1 and h_2 can be estimated. The above matrix can be written as

$$|T| = |A|^{-1}|B| \quad (17)$$

The temperature vector may be solved by matrix inversion. However, it can be solved in the present study by MATLAB program. To find h_1, h_2 and Nu correlations employed for forced convection (flat plate, constant temperature) [1] are:

$$Nu_x = \frac{1}{\sqrt{\pi}}\sqrt{Re_x} \cdot \frac{Pr}{(1+1.7\,Pr^{1/4}+21.36\,Pr)^{1/6}} \quad \text{and} \quad Nu_{m,lam} = 2\,Nu_x \quad (18)$$

At laminar, $Re_x < 5 \times 10^5$

$$Nu_{m,tur} = \frac{0.037\,Re_x^{0.8}\,Pr}{1+2.443\,Re_x^{-0.1}\,(Pr^{2/3}-1)} \quad (19)$$

At turbulence, $5 \times 10^5 < Re_x < 10^7$, $0.6 < Pr < 2000$

$$Nu_m = \sqrt{Nu_{m.lam}^{\,2} + Nu_{m,tur}^{\,2}} \quad (20)$$

Correlations employed for natural convection (flat plate, constant temperature) [12] are:

$$Nu_m = 0.54\,Ra^{1/4} \quad (21)$$

At $10^4 < Ra < 10^7$, upper heated horizontal surface

$$Nu_m = 0.14\,Ra^{1/3} \quad (22)$$

At $10^7 < Ra < 10^{11}$, upper heated horizontal surface

$$Nu_m = 0.27\,Ra^{1/4} \quad (23)$$

At $10^5 < Ra < 10^{10}$, lower heated horizontal surface

2.3 Chimney

The chimney converts the thermal energy produced by the solar collector into kinetic energy. The density difference, which is created by the rise in temperature in the collector works as the driving force, presented as Δp_{tot}. The heat transfer taking place across the chimney section surface is negligible. Applying the energy equation across a differential section of the chimney as shown in Fig. 3 yields.

$$\frac{d\rho w^2}{dz} = -\frac{dp}{dz} - (\rho - \rho_0)g \tag{24}$$

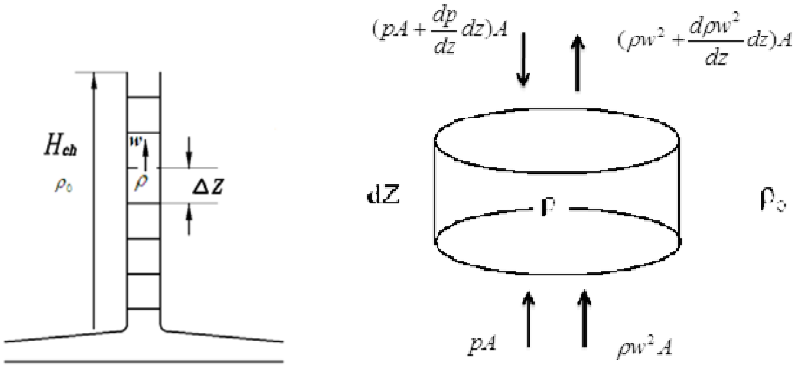

Fig. 3: Applying momentum equation on an element of the chimney

Thus the velocity at chimney outlet (at turbine resealed) can be expressed as

$$w = \sqrt{\frac{2}{\rho}\left[\int_0^{H_k} (\rho_0 - \rho)gdz - \Delta p_{friction}\right]} \tag{25}$$

Outside of the chimney; temperature, pressure, and density variation of air is calculated considering the standard atmosphere relationships

$$T_\infty(z) = T_\infty(0)\left(1 - \frac{k-1}{k}\frac{z}{H_0}\right)$$

$$P_\infty(z) = P_\infty(0)\left(1 + \frac{k-1}{k}\frac{z}{H_0}\right)^{K/(K-1)}$$

$$\rho_\infty(z) = \rho_\infty(0)\left(1 + \frac{k-1}{k}\frac{z}{H_0}\right)^{1/(K-1)} \tag{26}$$

With

$$H_0 = \frac{R \cdot T_\infty(0)}{g} \tag{27}$$

And k=1.235(standard atmosphere). Temperature, pressure, and density variation of air inside the chimney are calculated considering an adiabatic expansion process. Replacing k=1.235 by γ=1.4005 and subscript ∞ by t, they can be estimated from the equations (26) at any Z and t.

Velocity at any section across chimney is calculated by applying continuity equation under steady state condition. Moreover correlations employed for the friction in the chimney (assuming smooth pipe) for both laminar and turbulent flow are considered as edited in [13].

2.4 Turbine and Generator

In Ref. [14] work, the pressure drop of the turbine at the optimal proportion of the total pressure difference was calculated at 2/3 (i.e., 12.5% more than for a free-standing wind turbine, where this proportion is given by the Betz factor as $\left(\frac{\Delta p_{tur}}{\Delta p_{tot}}\right)$ = 16/27). Thus, this constant pressure drop assumption led to overestimating the size of the flow passages in the plant and somewhere the power output. According to Ref. [10], the maximum factor of pressure drop $\left(\frac{\Delta p_{tur}}{\Delta p_{tot}}\right)_{max}$ is calculated at each time step as:

$$\left(\frac{\Delta p_{tur}}{\Delta p_{tot}}\right)_{max} = \frac{n-m}{n+1} \tag{28}$$

Considering that ***n*** which is the power of volume flow in chimney that makes the loss pressure due to friction, is proportional with it, which selected as 1.75 according to relation of volume flow rate with pressure loss at turbulence regime. Also, m is the negative power of volume flow that makes the potential pressure is proportional with it, which calculated by:

$$m = -\frac{\eta_{coll}}{\alpha_{absor}} \tag{29}$$

The maximum available power can be calculated by the following equation.

$$P_{th\,max} = \left(\frac{\Delta p_{tur}}{\Delta p_{tot}}\right)_{max} . \Delta p_{tot} . V . A \tag{30}$$

And the output power obtained according to turbine efficiency by:

$$\mathbf{P_{out}} = \eta_{tur} \cdot \mathbf{P_{th,\,max}} \tag{31}$$

The theoretical model assumes that for a short collector, the temperatures of the ‘‘boundaries’’ surrounding the air streams are uniform and the temperatures of the air streams vary linearly along the collector. A long collector can be assumed to be divided equally into a finite number of short collectors, or sections. The wall and mean air temperatures of the first section are equal to the ambient temperature. Heat transfer coefficients are evaluated according to the initially guessed values. An iterative process is then created and the mean temperatures for the section calculated using the equations derived by employing a standard package matrix-inversion. The inlet air temperature of the next section is set equal to the outlet temperature of the last section. The iterative process is repeated until all consecutive mean temperatures differ by less than a desired value.

3. RESULTS AND DISCUSSION

First the mathematical model is validated with the actual accurate measured data visualizing real time performance. The plant of Manzanares can be considered as a reference of that area with the required data. It has about 122 m collector radius with height 1.85 m, 194.6 m chimney height and 2.08 m chimney radius where the turbine has 5 m with four blades. The model is validated with the data measured from the plant. After validation the chimney performance is studied for different effective parameters.

3.1 Validation of the Numerical Simulation

To validate the mathematical model, the theoretical performance data obtained by the program were compared with the experimental data of the plant installed in Manzanares, Spain (1982) edited by [15] under the same weather conditions.

The estimated data is compared with that was measured for Manzanares at Sep. 2, 1982. A comparison between numerically estimated and measured air temperature difference at center of collector is given in Fig. 4. The results showed a maximum difference of 5 degrees at the early hours. This difference may be due to the assumptions used in the model such as the model assumed that the first element has the ambient temperature.

Moreover constant and uniform cover and ground (absorber) properties are assumed. Also the assumption of radial uniform flow under the collector depends to a great extend on the wind direction especially in the case of the experimental study on a model reduced in dimension.

Fig. 5 illustrates the estimated and measured velocity at entrance of chimney. The calculated velocity was in close agreement with those obtained experimentally. The average difference over the day-time was in most within 1m/s. Similarly as explained for Fig. 4 that difference is caused by assuming that the first-element temperature of the collector equals the ambient one and the ambient temperature is low in the early morning.

Fig. 6 illustrates the numerical and measured pressure difference produced across chimney due to densities difference from bottom to top of chimney, the large difference between numerical and measured pressure in the readings before 9 o'clock and after 13 o'clock may be attributed to the fact that occurred, air flow through chimney was considered adiabatic through each element. While actually at the morning of day, the updraft air has been hotter than the chimney body, so that, a part of energy of air is transferred from air to chimney's body. This energy transferred mainly decreases the potential pressure produced across chimney because the air at top of chimney will not be hotter enough than the ambient air at same level. Vice versa is true, at the evening of day, the chimney has been hotter than the updraft air, so that this air has been got an additional energy which increases the potential pressure across chimney because the air at top of chimney hotter than the ambient air at same level.

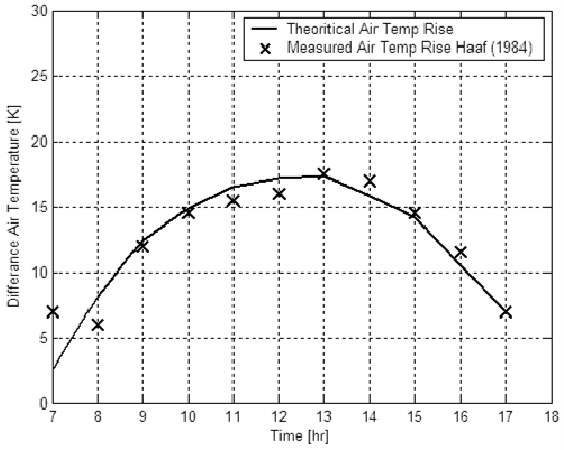

Fig. 4: Theoretical and measured air temperature difference (at center of collector)

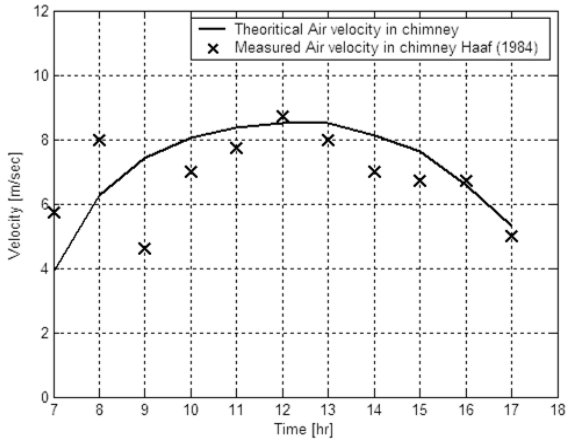

Fig. 5: Theoretical and measured velocity at entrance of chimney

The third view of validation was carried out by comparing the results of the present collector efficiency of analytical and experimental with those published by [15].

Collector efficiency is calculated by using equation (5.5), beside that it can be used to validate the mass flow rate across the solar chimney system.

$$\eta_{coll} = \frac{cp\,.m^{\cdot}.\Delta T}{\pi.{R_{coll}}^2.I_{tot}} \tag{32}$$

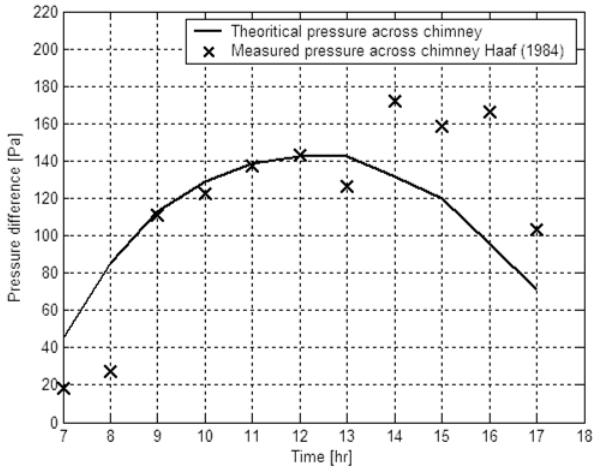

Fig. 6: Theoretical and measured pressure difference across chimney

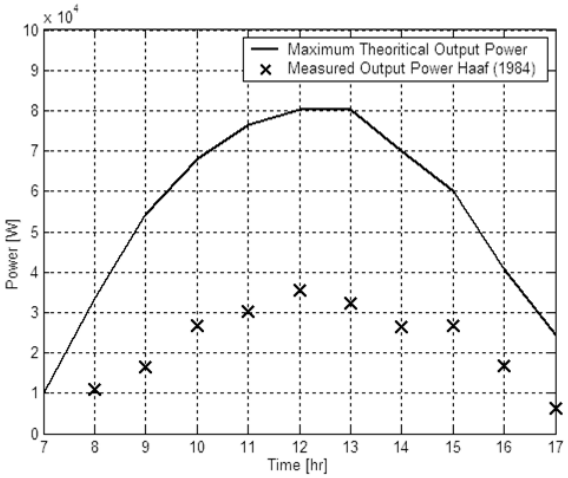

Fig. 7: Maximum available power and experimental output power

The surface conductivity k_{ground} (0.1 to 0.7$W/m.K$) has a pronounced effect on the 24-hour pattern of collector efficiency. In the analytical model, the surface conductivity is used as thermal property of ground and kept constant at 0.6 *W/m.K.* The theoretical daily mean collector efficiency is 31% approximately; it's closed to measured value as published by [15] which is 31.3 %.

The experimental terminal power (output power P_{out}) and the potential power (max. theoretical power $P_{th\,max}$) – which calculated from the maximum pressure difference across turbine to the total pressure difference across the chimney-is shown in Fig. 6. It is noted that, the maximum theoretical power and measured power are not validated as illustrated in Fig. 7. Perhaps that is obtained from the dust and some parameters those are not considered in the mathematical model. Finally the hourly variation of the temperature, velocity, pressure difference and power are completely similar to the normal variation of the solar radiation.

3.2 Influences of the Geometrical Dimensions

To have a general view of how the performance of a solar chimney power plant may be affected by varying the geometrical dimensions, basically chimney's height, chimney's radius and collector radius. The basic dimensions used in the model that the variable dimensions referred to them are 2050 m collector radius, 1000 m chimney height and 60 m chimney radius.

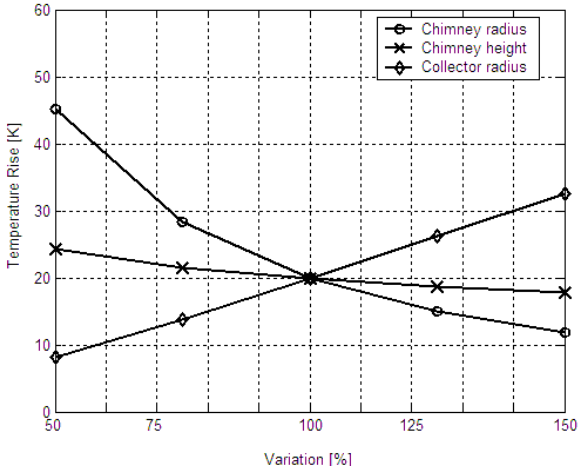

Fig. 8: The influence of geometrical dimensions on the maximum rise temperature

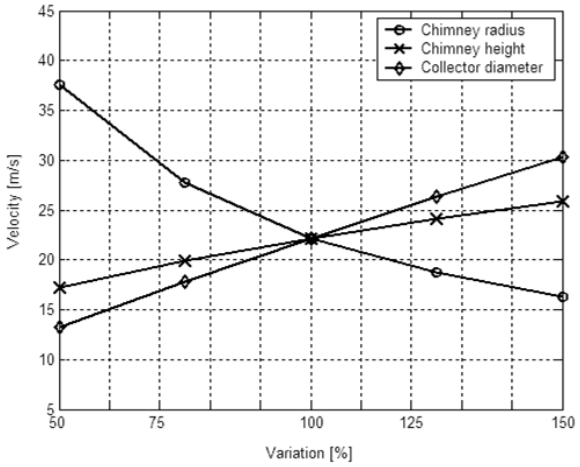

Fig. 9: The influence of geometrical dimensions on the maximum chimney velocity

As indicated in Fig. 8 and 9 the velocity and temperature relationship with the chimney radius and collector radius are relatively the same. The chimney height effect is slightly different on the temperature and velocity. Increasing the chimney radius and height improves the temperature and velocity. Similarly in Fig. 8 and 9, the chimney geometry has a significant effect on the chimney plant power. That effect is reduced in the case of pressure ratio as presented in Fig. 10.

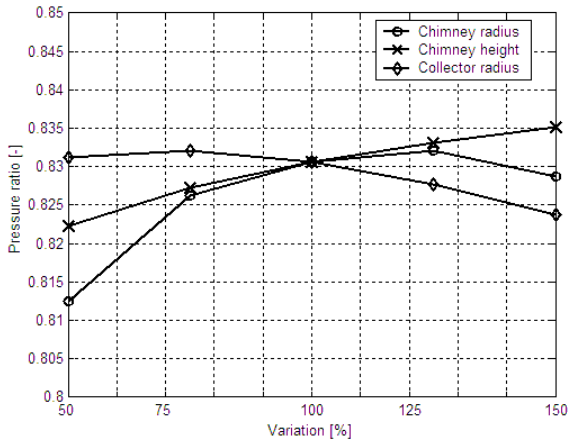

Fig. 10: Influence of geometrical dimensions on the maximum pressure ratio

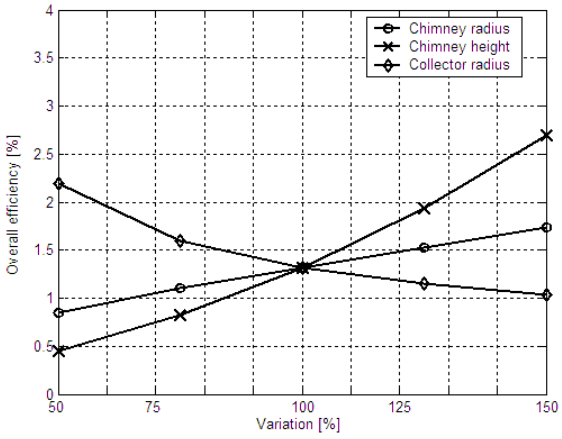

Fig. 11: The influence of geometrical dimensions on the minimum overall efficiency

Accordingly variation effect of the chimney geometry on the efficiency is significant. Perhaps the chimney height has more effect that the radius. On the other hand the collector radius effect is not significant.

The comparisons between the influences of solar chimney dimensions are illustrated in Tab. 1. The influences of chimney height on the available power and energy produced per day are higher than influences of collector radius and chimney radius. The variation of available power is 0.3 MW/m which is corresponding to 1 MW per 0.33% of

chimney height increase relative to basic model. The variation of energy produced is 2.78 (MW.h/day)/m which is corresponding to 1 GW.h/day per 0.36% of chimney height increase relative to basic model. Also, the influence of chimney height on overall efficiency has a higher effect by 0.022 %/m which is corresponding to 1 % per 0.46 % of chimney height increase relative to basic model as illustrated in Tab. 1. That means if solar chimney is used as a power plant it is useful to be installed with high chimney to increase the power produced and efficiency.

The influences of collector radius on the temperature are higher than influences of chimney radius and chimney height. That according to the variation of temperature is $12x10^{-3}$ ^{o}C/m which is corresponding to 1^{o}C per 4% of collector radius increase relative to basic model. But the temperature decreased by the chimney radius and chimney height increase. That means if solar chimney is used as dryer it is useful to use large collector area and the temperature under collector. That can improve the chimney efficiency.

The influences of chimney radius on the mass flow rate and the overall efficiency are higher than influences of collector radius and chimney height, but the overall efficiency is minor parameter at design.

Tab. 1: Comparison of influences of the chimney dimensions

	Chimney height	**Collector radius**	**Chimney radius**
Temperature rise rate [^{o}C/m]	$-6.25x10^{-3}$	$+12x10^{-3}$	-0.5
Available power rate [MW/m]	+0.3	+0.12	+1.8
Energy produced per day rate [(MW.Hr)/m]	+2.78	+0.93	+3.3
Mass flow rate [(ton/s)/m]	+0.09	+0.09	+5
Overall efficiency rate [(%)/m]	+0.022	$-0.56x10^{-3}$	+0.016

Another analysis to obtain the optimum dimensions. A power is selected as 200 MW and corresponding to 1.75 GW.h/day for 11 sunny hours, three power plants with different dimensions are selected, each one produces same power and energy.

Tab. 2: Dimensions of solar plants, each one produces 200 MW

	Plant (1)	**Plant (2)**	**Plant (3)**
Collector Radius	2250 m	2050 m	2050 m
Chimney Height	1000 m	1090 m	1000 m
Chimney Radius	60 m	60 m	72 m

The differences of three plants is in one dimension where;

- Plant (1) has large collector radius.
- Plant (2) has highest chimney.
- Plant (3) has large chimney radius.

As illustrated in Tab. 3 plant (1) has slightly more efficiency than the other two plants. Moreover it has the highest temperature rise. That conclusion cannot be generalized because there is a reference value for each dimension. Therefore the optimum plant's dimensions cannot be determined physically, however, the comparison of performance parameters of these plants is illustrated. But the economic view and the technology of installation are the main parameters to select which of these dimensions is optimum.

Tab. 3: Comparison of performance parameters of plants produced 200 MW

	Plant (1)	Plant (2)	Plant (3)
Temperature rise [^{o}C]	24	18	16
Mass flow [ton/s]	270	260	300
Overall efficiency [%]	2	1.5	1.45

3.3 Performance of large scale solar chimney

According to literature survey, the solar chimney power plant is more economic, if the plant is in large scale, so that, the basic geometrical dimensions were selected to achieve this goal. Similar dimensions are used as considered in a previous study by [1]**.** The main dimension and specifications are indicated in Tab. 4. Annual measured data of metrological data are used.

Fig. 12 presents the maximum available power verses the months of the year. It is noted that the maximum available power varies over the year and it has a maximum of 190 MW in June (summer) and a minimum of 87 MW in January (winter), i.e. it has values at winter decrease by factor of half than in summer.

Fig. 13 presents the overall efficiency corresponding to maximum power. The corresponding time of minimum overall efficiency is the maximum available power, that because it is reversely to solar radiation. It is noted that the overall efficiency corresponding to maximum available power does not increase than 2%, that also agreements to literature [4].

Tab. 4: Technical data and design criteria of the a solar chimney power plant

Parameters	Value	Unit
Chimney height	1000	[m]
Chimney radius	60	[m]
Mean collector radius	2050	[m]
Canopy height at inlet	3.5	[m]
Canopy height at outlet	35	[m]
Cover material	PVF plastic sheet	-
Time step	3600	s
Number of radial collector sections	300	-
Cover emissivity	0.1	[-]

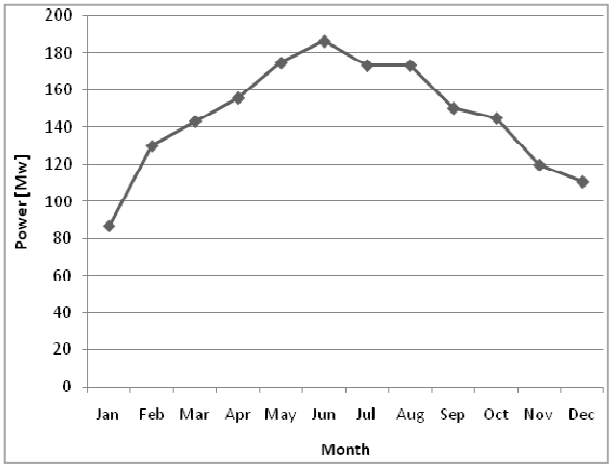

Fig. 12: Annual variation of the power produced by the chimney plant

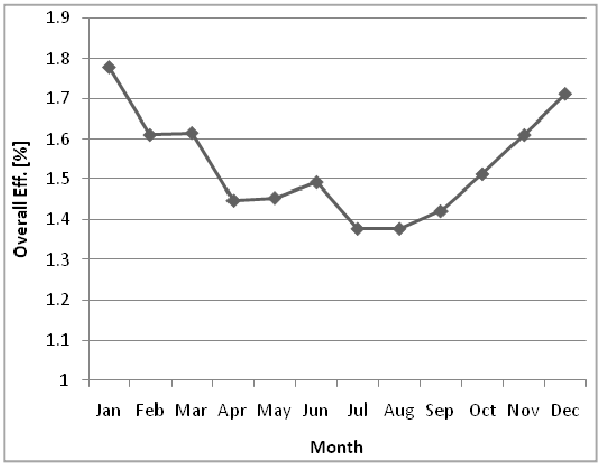

Fig. 13: Annual variation of the overall efficiency corresponding to maximum power

4. CONCLUSION

The main objective of this work is to investigate the performance of a solar chimney power plant under local climate condition of Egypt. A validated numerical simulation of the solar chimney has been developed. A comparison between the numerical and experimental performance has been investigated to validate the numerical simulation. The mathematical model has been used to predict of performance of solar chimney power plant over a year in Egypt and study the effects of geometrical parameters. It was found that the chimney height has the highest influence on the both chimney power and efficiency where the collector radius raises the temperature inside the collector. Accordingly the annual performance of a large-scale chimney power plant was demonstrated under the weather conditions of Egypt with a great potential of such technology.

REFERENCES

[1] Bernardes, M. A., Dos, S., Vob, G., Weinrebe, A. (2003). Thermal and technical analyses of solar chimney. *Int. J Solar Energy*, (75), 511–524.

[2] Mullett, L. B. (1987). The solar chimney – overall efficiency, design and performance. *Int. J Ambient Energy*, (8), 35-40.

[3] Pasumarthi, N., Sherif, S. A. (1998). Experimental and theoretical performance of a demonstration solar chimney model-part i: mathematical model development. *Int. J Energy Res*, (22), 277–288.

[4] Bilgen, E., Rheault, J. (2005). Solar chimney power plants for high latitudes. *Int. J Solar Energy,* (79), 449-458.

[5] M. Tingzhen, L. Wei, X. Guoling, X. Yanbin, G. Xuhu, P. Yuan (2008). Numerical simulation of the solar chimney power plant systems coupled with turbine. *Renewable Energy*, (33), 897–905.

[6] Gannon, A. J., Backström, T. W. (2000). Solar chimney cycle analysis with system loss and solar collector performance. *Journal Of Solar Energy Engineering*, (122), 133–137.

[7] Fluri, T. P., Backström, T. W. (2008). Performance analysis of the power conversion unit of a solar chimney power plant, *Int. J Solar Energy*, (82), 999–1008.

[8] Padki, M. M., Sherif, S. A. (1999). On a simple analytical model for solar chimneys. *Int. J Energy Res,* (23), 345-349.

[9] Bernardes, M. A., Dos, S., Backström, T. W., Kröger, D. G. (2009). Analysis of some available heat transfer coefficients applicable to solar chimney power plant collectors. *Int. J Solar Energy*, (83), 264–275.

[10] Backström, T. W., Fluri, T. P. (2006). Maximum fluid power condition in solar chimney power plants – an analytical approach. *Int. J Solar Energy,* (80), 1417-1423.

[11] Maia, C. B., Ferreira, A. G., Valle, R. M., Cortez, M. F. B. (2009). Theoretical evaluation of the influence of geometric parameters and materials on the behavior of the airflow in a solar chimney. *Computer & Fluid*, (38), 625–636.

[12] Zhou X., Yang J., B. Xiao, G. Hou and F. Xing (2009). Analysis of chimney height for solar chimney power plant. *Applied Thermal Engineering,* (29), 178–185.

[13] Incropera, F. P., D. P. De Witt (2002). *Fundamentals of heat and mass transfer* (5th edition). New York: John Wiley and Sons.

[14] Haaf, W., Friedrich, K., Mayer, G., Schlaich, J. (1983). Solar chimneys part i: principle and construction of the pilot plant in manzanares. Solar Chimneys, *Int. J Solar Energy,* (2), 3–20.

[15] Haaf, W. (1984). Solar chimneys part II: preliminary test results from manzanares pilot plant. Solar Chimneys, *Int. J Solar Energy*, (2), 141–16.